1 Modeling Approach

1.1 Intersection Points & Coefficient Matrix

In each tetrahedral element $\mathcal{V}_k$, we locate six intersection points q_j by ray-casting from the **barycenter** x_b along the three anisotropy axes to the faces. At the same time we build a 4×6 coefficient matrix C^k whose entries let us reconstruct any intersection q_j from the four vertex positions.

1. **Barycenter**

   where x_i are the four vertex coordinates.

$$x_b \;=\; \frac{1}{4}\sum_{i=1}^{4} x_i \tag{2.22}$$

2. **Point-in-triangle test & barycentric coords**

   A traced point q_j on face $\Delta_{i_1 i_2 i_3}$ is inside if and only if

$$S_{\Delta_{i_1 i_2 i_3}} \;=\; S_{\Delta_{q_j\, i_2\, i_3}} + S_{\Delta_{i_1\, q_j\, i_3}} + S_{\Delta_{i_1\, i_2\, q_j}}. \tag{2.23}$$

   Then its local (area) coordinates on that triangle are

$$\xi = \frac{S_{\Delta_{q_j\, i_2\, i_3}}}{S_{\Delta_{i_1 i_2 i_3}}}, \quad \eta = \frac{S_{\Delta_{q_j\, i_1\, i_3}}}{S_{\Delta_{i_1 i_2 i_3}}}, \quad 1 - \xi - \eta = \frac{S_{\Delta_{i_1\, i_2\, q_j}}}{S_{\Delta_{i_1 i_2 i_3}}}. \tag{2.24}$$

3. **Building the coefficient matrix C^k**

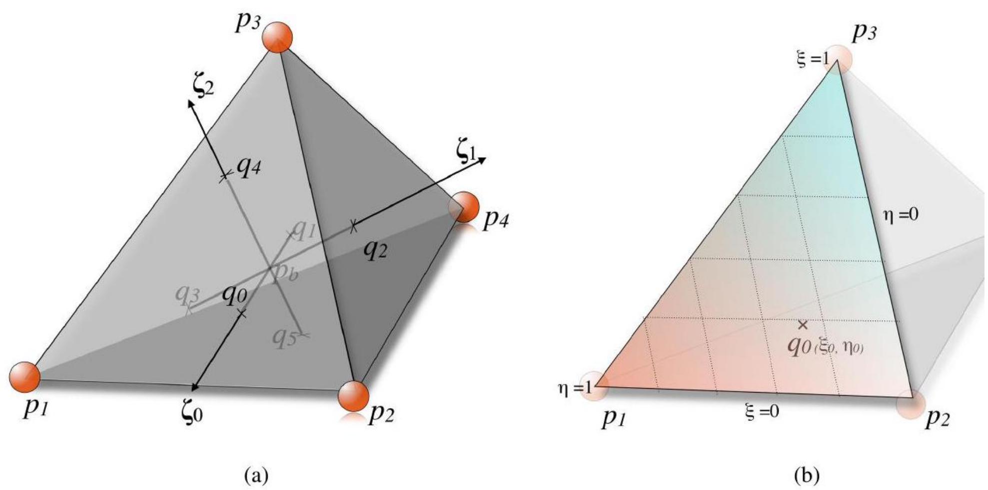

Figure 1: Intersection points in a tetrahedral volume element: The tetrahedron with three axes of anisotropy set at the barycenter and the six intersection points that they define (a), a triangular face of the element containing an intersection point and the coefficients ξ_0 and η_0 related to the intersection point. Note that ξ increases with the cyan color gradient starting from $\xi = 0$ at the line segment (p_1, p_2) and is equal to $\xi = 1$ at p_3, while η increases along the orange color gradient starting from $\eta = 0$ at (p_2, p_3) until it reaches $\eta = 1$ at p_1 (b).

For each intersection q_j we evaluate the four linear shape-functions N_i of the tetrahedron's nodes

$i = 1 \dots 4$. On the face containing q_j, those coincide with the barycentric coordinates:

$$\begin{cases} N_{i_1}(q_j) = 1 - \xi - \eta, \\ N_{i_2}(q_j) = \xi, \\ N_{i_3}(q_j) = \eta, \\ N_{i_4}(q_j) = 0, \end{cases}$$

where $\{i_1, i_2, i_3\}$ are the face nodes and i_4 is the opposite vertex. We then set

$$C^k_{ij} \;=\; N_i\big(q_j\big),$$

assembling a 4×6 matrix whose j-th column holds the four shape-function values at q_j.

4. **Updating intersections**

   At runtime, once the current vertex positions x^t_i are known, each intersection moves as

$$x^t_j \;=\; \sum_{i=1}^{4} C^k_{ij}\, x^t_i \tag{2.25}$$

   reproducing the straight-sided mapping of a linear tetrahedron.

   In the implementation the six q_j and the corresponding C_k are updated each step to remain exact under large deformation.

1.2 Internal Forces

Internal ("deformation") forces in each tetrahedron are computed by **three axial springs** along the anisotropy axes, plus **three torsion springs** coupling each pair of axes. See Fig. 2. The angle α^t_{lm} between the axes ζ_{l} and ζ_{m} can be given by...

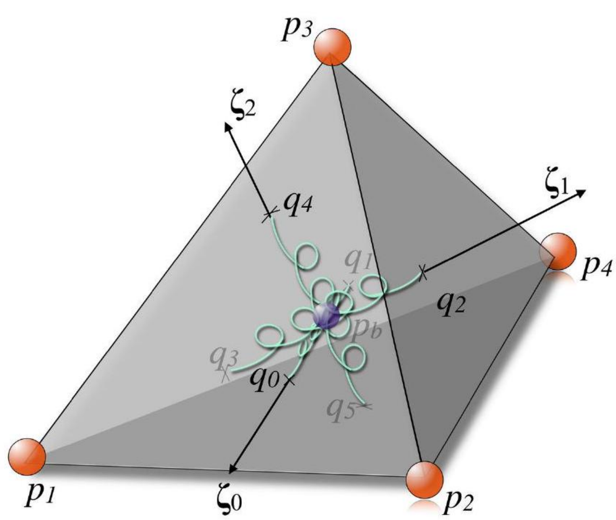

Figure 2: A tetrahedron with three axial springs (in cyan) along the axes of anisotropy and three torsion springs in the barycenter of the tetrahedron (in violet).

1.2.1 Axial Springs

- **Axis vectors**: Along axis $\ell \in \{1,2,3\}$, let the two intersection points be $q_{\ell,1}$ and $q_{\ell,2}$. Their current axis vector is
$$\zeta_\ell^t = x_{q_{\ell,1}}^t - x_{q_{\ell,2}}^t.$$
- **Initial length** (at $t=0$):
$$l_\ell^0 = \|\zeta_\ell^0\| = \left\| x_{q_{\ell,1}}^0 - x_{q_{\ell,2}}^0 \right\|. \tag{2.30}$$
- **Unit direction**:
$$\hat{\zeta}_\ell^t = \frac{\zeta_\ell^t}{\|\zeta_\ell^t\|}. \tag{2.31}$$
- **Hooke's law** (linear axial force):
$$\boxed{f_{\ell,\,\mathrm{axial}}^t = -\,k_\ell\big(\|\zeta_\ell^t\| - \|\zeta_\ell^0\|\big)\,\hat{\zeta}_\ell^t} \tag{2.35}$$
where k_ℓ is the stiffness constant.

1.2.2 Torsion Springs

To capture bending resistance between each pair of anisotropy axes in a tetrahedron, we introduce **torsion springs**. These springs penalize deviations of the angles between axes from their rest values.

1. Angle between two axes For any two axes ℓ and m, the angle is

$$\alpha_{\ell m}^t = \arccos\big(\hat{\zeta}_\ell^t \cdot \hat{\zeta}_m^t\big), \quad \alpha_{\ell m}^0 = \alpha_{\ell m}^{t=0} \tag{2.32}$$

where $\hat{\zeta}_\ell^t$ and $\hat{\zeta}_m^t$ are the unit–direction vectors at time t, and $\alpha_{\ell m}^0$ is the **rest angle**, measured in the undeformed configuration.

2. Decomposing the torsion force At each intersection point on axis ℓ, the net torsion force $f_{\ell,1}$ splits into three orthogonal components:

$$f_{\ell,1} = f_S(\zeta_\ell, \alpha_{\ell m}, \alpha_{\ell n})\,\hat{\zeta}_\ell + f_\tau(\zeta_\ell, \alpha_{\ell m}, \alpha_{\ell n})\,\hat{\zeta}_m + f_\tau(\zeta_\ell, \alpha_{\ell m}, \alpha_{\ell n})\,\hat{\zeta}_n, \tag{2.33}$$

with $f_{\ell,2} = -\,f_{\ell,1}$, and $\{m,n\}$ are the other two axes.

- **Axial** component f_S acts along $\hat{\zeta}_\ell$.
- **Torsional** components f_τ lie in the planes $(\hat{\zeta}_\ell, \hat{\zeta}_m)$ and $(\hat{\zeta}_\ell, \hat{\zeta}_n)$.

Expressions for f_S and f_τ We derive both from simple spring energies: $f_S = -\frac{\mathrm{d}U_S}{\mathrm{d}\|\zeta_\ell\|}$.

In a conservative spring model, the force along a single coordinate x is the negative derivative of its potential energy:
$$F(x) = -\frac{\mathrm{d}}{\mathrm{d}x}\,U(x).$$
Here our "coordinate" is the current length $\|\zeta_\ell\|$, so the axial force magnitude is
$$f_S = -\frac{\mathrm{d}}{\mathrm{d}\|\zeta_\ell\|}\,U_S.$$

1. **Axial term**: Define $U_S = \frac{1}{2}\,k_\ell\big(\|\zeta_\ell^t\| - \|\zeta_\ell^0\|\big)^2$. Then

$$f_S = -\,\frac{\mathrm{d}}{\mathrm{d}\|\zeta_\ell\|}\Big[\tfrac{1}{2}\,k_\ell(\|\zeta_\ell\| - \|\zeta_\ell^0\|)^2\Big] = -\,k_\ell\big(\|\zeta_\ell^t\| - \|\zeta_\ell^0\|\big),$$

and the vector is $\mathbf{f}_S = f_S\,\hat{\zeta}_\ell$.

2. **Torsional terms**: Define $U_\tau = \frac{1}{2}\sum_{p\in\{m,n\}} k_{\ell p}\,\big(\alpha_{\ell p}^t - \alpha_{\ell p}^0\big)^2$. Differentiating with respect to each angle gives

$$f_\tau(\zeta_\ell, \alpha_{\ell m}, \alpha_{\ell n}) = -\,k_{\ell m}\,\big(\alpha_{\ell m}^t - \alpha_{\ell m}^0\big),$$

and similarly for (ℓ, n).

3. Linear torsion-spring model

$$\boxed{f_{\ell\to m}^t = -\,k_{\ell m}\,\big(\alpha_{\ell m}^t - \alpha_{\ell m}^0\big)\,\hat{\zeta}_m^t,}\quad f_{m\to\ell}^t = -\,f_{\ell\to m}^t. \tag{2.40–2.41}$$

4. Cosine-approximation (small-angle) When axes remain near orthogonal, $\alpha_{\ell m}^t - \alpha_{\ell m}^0 \approx (\hat{\zeta}_\ell^t\cdot\hat{\zeta}_m^t) - (\hat{\zeta}_\ell^0\cdot\hat{\zeta}_m^0)$. Thus

$$\boxed{f_{\ell\to m}^t = -\,k_{\ell m}\,\big((\hat{\zeta}_\ell^t\cdot\hat{\zeta}_m^t) - (\hat{\zeta}_\ell^0\cdot\hat{\zeta}_m^0)\big)\,\hat{\zeta}_m^t,}\quad f_{m\to\ell}^t = -\,k_{\ell m}\,\big((\hat{\zeta}_\ell^t\cdot\hat{\zeta}_m^t) - (\hat{\zeta}_\ell^0\cdot\hat{\zeta}_m^0)\big)\,\hat{\zeta}_\ell^t. \tag{2.44–2.45}$$

Assembly Each tetrahedron contributes:

- 6 axial-spring forces, and
- 6 torsion-spring forces,

which are then distributed to the four vertices via the shape-function coefficients C^k and summed with any body forces before time integration.

1.3 Simplified Volume Preservation (Barycentric Volume Springs)

To control tetrahedral volume without full tensors, we use **barycentric springs** [Eqns. 2.76–2.77]:

1. **Current barycenter**:

$$x_b^t = \frac{1}{4}\sum_{i=1}^{4} x_i^t.$$

2. **Radial vectors**: $\xi_j^t = x_b^t - x_j^t$, with lengths $\|\xi_j^t\|$.
3. **Rest lengths** $\|\xi_j^0\|$ computed at $t = 0$.
4. **Total length error**:

$$\Delta L = \sum_{j=1}^{4}\|\xi_j^t\| \;-\; \sum_{j=1}^{4}\|\xi_j^0\|.$$

5. **Barycentric spring force** on node j:

$$f_j^t = -\,k_s\,\Delta L\,\frac{\xi_j^t}{\|\xi_j^t\|} \;-\; c\,(v_j^t - v_b^t),$$

where k_s is the bulk-modulus-based stiffness, c a damping coefficient, and v_b^t the barycenter velocity.

6. **Adaptive stiffness update** (LMS, Eq. 2.81):

$$k_s^{t+\Delta t} = k_s^t + \mu \, \Delta V \sum_{j=1}^{4} \|\xi_j^t\|,$$

clamped to $[k_{\min}, k_{\max}]$, with $\Delta V = V^t - V^0$ the volume error.

This completes the fully-spring-based model:

1. mesh topology & intersection (Eqs. 2.22–2.25),
2. internal forces via axial+torsion springs (Eqs. 2.30–2.44–2.45),
3. volume control via barycentric springs.

To do list: 1. survey the